

Multiscale modeling of virus replication and spread

Peter Kumberger^{1,2}, Felix Frey^{1,3}, Ulrich S. Schwarz^{1,3} and Frederik Graw^{1,2}

¹ BioQuant-Center, Heidelberg University, Germany

² Center for Modeling and Simulation in the Biosciences (BIOMS), Heidelberg University, Germany

³ Institute for Theoretical Physics, Heidelberg University, Germany

Correspondence

Frederik Graw and Ulrich Schwarz,
BioQuant-Center, Heidelberg University, Im
Neuenheimer Feld 267, 69120 Heidelberg,
Germany
Fax: +49 (0)6221 54 9331
Tel: +49 (0)6221 54 51309; +49 (0)6221 54
9399
E-mails: frederik.graw@bioquant.
uni-heidelberg.de; ulrich.schwarz@bioquant.
uni-heidelberg.de

(Received 20 December 2015, revised 21
January 2016, accepted 7 February 2016)

doi:10.1002/1873-3468.12095

Edited by Wilhelm Just

Replication and spread of human viruses is based on the simultaneous exploitation of many different host functions, bridging multiple scales in space and time. Mathematical modeling is essential to obtain a systems-level understanding of how human viruses manage to proceed through their life cycles. Here, we review corresponding advances for viral systems of large medical relevance, such as human immunodeficiency virus-1 (HIV-1) and hepatitis C virus (HCV). We will outline how the combination of mathematical models and experimental data has advanced our quantitative knowledge about various processes of these pathogens, and how novel quantitative approaches promise to fill remaining gaps.

Keywords: HCV; HIV; mathematical modeling; quantitative viral dynamics; systems biology

Viruses are systems biologists in the sense that they continuously explore which combinations of cellular processes might be exploited for successful replication and spread in a population of host cells. The resulting versatility and variability in their strategies mirror the complexity of the processes in the host and show the evolutionary capacity of pathogens to adapt. For example, human viruses such as the human immunodeficiency virus-1 (HIV-1) and hepatitis C virus (HCV) have found sophisticated ways involving the interaction of different cell surface receptors to realize cell entry to specific target cells [1]. Once inside the cell, molecular processes of viral transport, disassembly, integration, transcription, translation, assembly and, finally, export influence the efficiency of new virus production and, hence, viral spread. However, viral

spread is also influenced by the availability of target cells, cell motility, the surrounding tissue environment, and the proximity of counteracting immune responses. Thus, viral infection dynamics represents a complex process covering multiple scales in space and time whose understanding is a challenge to the modern biosciences (Fig. 1). Identification of the key factors involved, as well as a quantitative understanding of the various processes determining infection dynamics and disease outcome is needed to design appropriate treatment regimes.

Mathematical modeling is an essential tool to achieve a systems-level understanding of pathogen replication and spread. Analyzing patient data by mathematical models helped to identify the high replication rate of HIV-1 during the chronic infection

Abbreviations

AAV, adeno-associated virus; ART, antiretroviral treatment; BD, Brownian dynamics; EM, electron microscopy; HBV, hepatitis B virus; HCV, hepatitis C virus; HIV-1, human immunodeficiency virus-1; IFN- α , alpha interferon; MD, molecular dynamics; MTOC, microtubule organizing center; ODEs, ordinary differential equations; SMV, standard model of viral dynamics; SIV, simian immunodeficiency virus; TMV, tobacco mosaic virus; VSM, vesicular membrane structures.

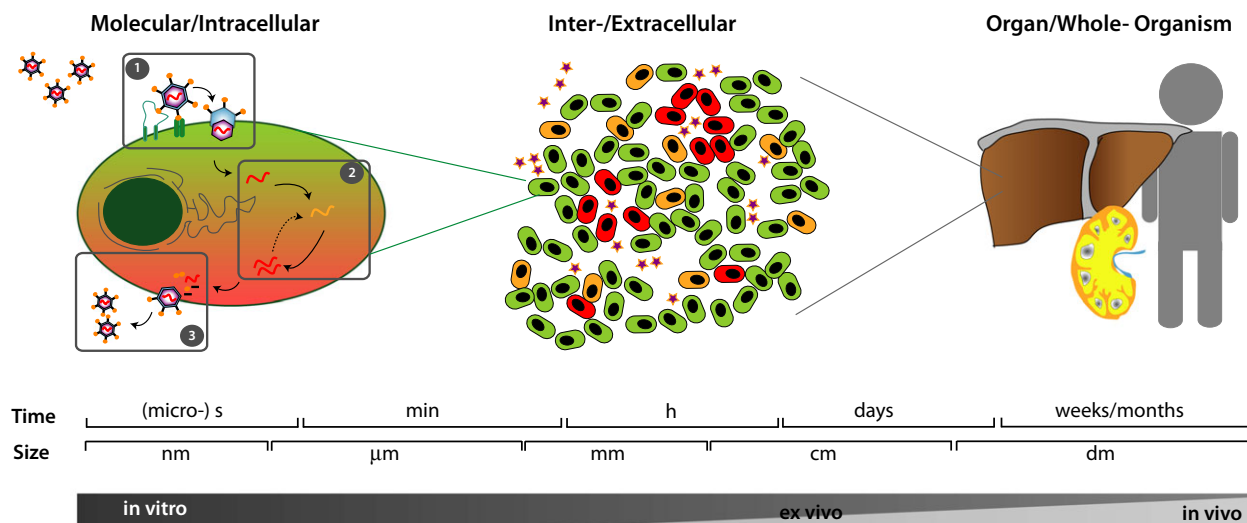


Fig. 1. Schematic of the different scales that are covered by processes of virus replication and spread. At the molecular and intracellular scales the main processes are viral entry (1), viral replication (2) and viral export (3). At the scale of a cell population looking at the spread of the pathogen, we distinguish between uninfected (green), infected (orange) and virus-producing infectious (red) cells. On the organismal scale, we deal e.g., with the infection of an organ, such as the liver, and the spread among organs. Dependent on the scale, different experimental techniques can provide quantitative information. Mathematical models help to integrate information from various scales and experimental models within a systematic and quantitative framework.

phase [2–4] and the mode of action of specific anti-HCV drugs [5,6]. In addition, computer simulations can help to understand the biophysical aspects of viral assembly and packaging and reveal rate limiting steps and physiological constraints [7]. Furthermore, mathematical models allow us to integrate information from different scales and experimental sources, and to examine processes that are not directly observable by experimental measurements, within a systematic and quantitative framework.

Advances in technologies for molecular and cell biology as well as imaging techniques improve our quantitative knowledge and can provide real life data of infection processes. For example in case of HCV infection, microscopy techniques have been developed to allow single-cell analysis of intracellular viral replication *in vitro* [8], to visualize infection dynamics within the liver of humanized mice [9], and to determine the infection status of single cells in liver biopsy samples of HCV-infected patients [10]. These new types of data provide valuable input for a systems-level understanding of pathogen replication and spread.

In the following, we will review various types of modeling techniques that, in combination with experimental data, have been used to determine and quantify processes of virus replication and spread across multiple scales. We will especially focus on viral infections caused by HIV-1 and HCV, and highlight how mathematical modeling has substantially

advanced our knowledge about the life cycle of these pathogens.

We will start by addressing the molecular processes of viral entry, transport and packaging individually (*Viral entry, transport and packaging*). Here, biophysical arguments play a major role regarding the dynamics of these processes. In a second step, we will look at the integrated process of viral replication within a cell (The replication within – intracellular processes) using population dynamic models. Going up in scale, we will introduce current and previous approaches on analyzing viral spread within tissues, and review results from within-host viral dynamics analyses, and their implications for intracellular dynamics (Viral spread at tissue levels – an integrated view). Our review will be concluded by a discussion of the future promises and challenges for an integrative analysis of pathogen replication and spread by novel experimental methods and observations (Conclusions and outlook).

Viral entry, transport and packaging

Crossing barriers and getting ahead

As viruses infect a host cell, they have to cross different barriers and exploit several host processes to get themselves transported from one compartment to another. Therefore, all viruses interact with cellular membranes and with the cytoskeleton, the dynamic

system of filamentous polymers that provides the large scale organization of the cell [11,12]. Different viruses have solved the challenge to move through the cell in different ways. In this sense, they form a group of systems biologists who know how to exploit the cellular transport system [13,14]. Through the recent advances in super resolution microscopy and single molecule imaging, it has now become possible to track the trajectories of viruses as they enter a cell, move through it and exit again [15,16]. A recent important step forward is the introduction of the CRISPR/Cas-system, which now makes it easier to mark the viral particles with appropriate fluorescent or chemical tags. At the same time, large advances have been made in marking membranes and cytoskeletal structures during live cell imaging, e.g., with silicon-rhodamine (SiR) derivatives for actin and tubulin [17], and in dynamically controlling the state of membranes and cytoskeleton, e.g., with optogenetics [18].

A viral infection starts with a viral particle binding to specific surface receptors of a host cell. The number of bound receptors necessary for cell entry, i.e., the stoichiometry of viral entry, varies strongly and is an important determinant of viral infectivity [19–21]. Moreover, sometimes these receptors are not easily accessible for the incoming virus and therefore it employs specific search strategies to find them, like e.g., murine leukemia virus (MLV) surfing along filopodia to entry sites at their base [22]. Most viruses cross the cell membrane by triggering endocytosis (including assembly of clathrin cages or caveolae) (Fig. 2), but some enveloped viruses simply fuse with the membrane. In this case, however, they also have to induce changes to the actin cortex underlying the plasma membrane, which is the second major barrier that has to be crossed at the cell periphery. Interestingly, HIV-1 has been reported to be capable of entry by both fusion and endocytosis [23]. Once inside the cell, viruses (and more so the endosomes in which they might be contained) are too large (size > 20 nm) as to simply diffuse through the cytoplasm (mainly due to obstruction by the actin cytoskeleton). Therefore, they have to exploit active transport by the host cell to get from the cell periphery where they enter to the region in which they replicate, such as the perinuclear region or the nucleus. For example, it has been shown by single-particle tracking that HIV-1 recruits dynein motors to be transported on the microtubule network toward the microtubule organizing center (MTOC) [24]. During this journey or when arriving close to a nuclear pore, the virus starts to uncoat and the genetic material is released. After replication and expression, the viral coat is assembled and the particle reverses its

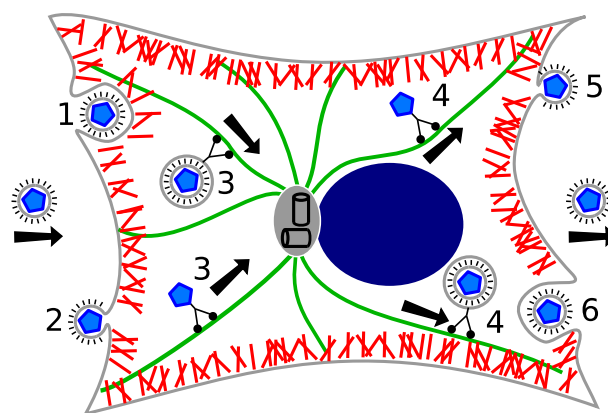


Fig. 2. Viral entry, exit, and transport strategies. To enter and exit, viruses (blue particles) have to overcome two physical barriers at the cell periphery: the plasma membrane (gray) and the actin cortex (red) underneath the plasma membrane. Enveloped viruses either enter via endocytosis (1) or membrane fusion (2). Once inside the cell, viruses make use of the intracellular transport system. By means of dynein motors (3) viruses are transported along microtubules (green) toward the microtubule organizing center (MTOC, crossed black cylinders). Newly assembled viruses are transported along microtubules by kinesin motors (4) toward the actin cortex, where they exit, e.g., via budding (5) or exocytosis (6).

course. For cell exit, viruses can bud from the membrane, trigger exocytosis or simply lyse the host.

In general, the problem of virus arrival at the perinuclear region is a first passage problem in the theory of stochastic processes [25,26]. The most important reason for stochasticity is the number and type of motors that are recruited by the virus particle and the irregular kind of motion, which ensues thereafter. Other sources for stochasticity are the disordered organization of the cytoskeleton and the variability in the entry process. Once the corresponding mathematical equations have been formulated, they can be solved with the methods from stochastic dynamics, e.g., for the arrival at a small hole in the boundary [27]. Experimentally, a well-established model system for intracellular virus transport is an adeno-associated virus (AAV), which is also the most common vector for gene delivery and has been studied previously with single-particle tracking [28,29]. Several theoretical studies have addressed this system and established the typical time scales for the different stages of virus transport [26,30]. For example, it was reported that endocytosis might take 10 min, while the transport to the nucleus takes only 5 min and occurs with an efficiency of 90% [26]. However, another study reported longer time scales and a reduced efficiency [30].

Systems-level models for intracellular virus transport are challenging because they have to integrate different

specialized models each of which is already a challenge by itself. The best example for this important point is transport by multiple motors, which has been described by a large range of different models [31,32]. It has been pointed out from theoretical considerations that multiple motor transport is limited by stochastic loss of the connection to the cytoskeletal track [33]. Moreover, it has been shown that recruitment of motors that pull in different directions leads to a tug-of-war situation with large jumps in the stochastic trajectories [34]. Together, these effects lead to large variability in virus trajectories, as observed experimentally.

Virus entry through the plasma membrane has also been investigated in large detail from the modeling point of view [35,36]. As virus particles do not have any metabolism, it is assumed that this process has to proceed mainly by minimization of the total free energy, similar to the cellular uptake of nanoparticles [37]. The main driving force is assumed to result from the binding energy of the virus particle to the cell surface receptors, while the main resisting force is the bending energy of the plasma membrane. It is shown that for optimal particle sizes, indeed this physical picture can explain virus uptake. Similar considerations apply for exit by budding from the membrane [38].

Viral capsid assembly

Historically, two key findings have demonstrated that capsid assembly is strongly shaped by physical processes [39]. First, experimental observations that some viruses, such as the tobacco mosaic virus (TMV), can be assembled in a test tube [40] indicated that capsid assembly tends to be a physical process that does not consume energy. Second, Crick and Watson observed that viruses typically come as spheres or rods, because their shells are made from many identical subunits [41]. This insight was made more rigorous by Caspar and Klug through their classification scheme for icosahedral viruses (which constitute half of all known virus families) [42].

Physical considerations of viral capsid assembly do not only help to understand the underlying principles but they also demonstrate in which sense viruses are capable of beating physical constraints. After assembly, virus shells are much more stable than suggested by thermodynamics, indicating a process of maturation. A clear example is that of the HIV-1 capsid, which changes its shape from spherical to cone-like during maturation [43]. However, equilibrium considerations based on dissociation constants do not predict how capsid assembly proceeds dynamically, and how the system avoids to get trapped in intermediate assemblies. Moreover, it remains to be shown which

mechanisms have evolved to ensure capsid assembly in the heterogeneous and crowded environment of the host cell.

Experimentally, the dynamics of virus assembly was monitored mainly with small angle light and X-ray scattering [44]. However, these techniques can only give averaged values for the typical size of the intermediates as a function of time. In contrast, electron microscopy (EM) gives very detailed insight into the sizes and shapes of intermediates [45], but does not allow us to follow the dynamics. Nuclear magnetic resonance provides a tool to perform structure analysis of capsid proteins during capsid assembly, e.g., for HIV-1 [46]. Using single molecule techniques [47] or mass spectrometry one can investigate intermediate structures in the assembly process, e.g., for HBV or norovirus [48]. However, because each of these experimental approaches does only provide a glimpse on the overall process, mathematical models and computational simulations are essential to gain a systems-wide understanding.

From a systems biology point of view, it is important to develop methods that are able to simulate the complete process of capsid assembly. A large range of simulation approaches has been employed to study capsid assembly, as recently reviewed by Hagan [7]. At the current stage, no single approach is able to address all questions of interest at once, and, thus, the situation is similar to the experimental one, in which each new study provides a new piece for the overall puzzle.

The standard approach to model viral capsid assembly is the use of molecular dynamics (MD) simulations [47,49–51] including all relevant molecular interactions (van der Waals interactions, hydrogen bridges, ionic bridges, etc.) using software packages such as NAMD [52] or GROMACS [53]. The molecular structures of the assembling capsid proteins obtained by EM or X-ray scattering are deposited in the VIPER database [54]. MD-simulations allow the realistic implementation of protein–protein interactions [51,55], but come with a high computational cost. Therefore so far, the assembly process can only be studied over relative short timescales (typically $\sim 1 \mu\text{s}$) not allowing much statistical analysis.

There are several alternatives to all-atom MD-simulations (Fig. 3A) that are more computer-time efficient and therefore make it possible to simulate long time courses, including reversible dynamics. Early MD-studies used coarse-grained interaction rules and thus allowed one to simulate capsid assembly with a statistical analysis of its intermediates (Fig. 3B) [47,49]. Alternatively, one can use such coarse-grained models for Monte Carlo simulations (which sample only the most important configurations according to a Boltz-

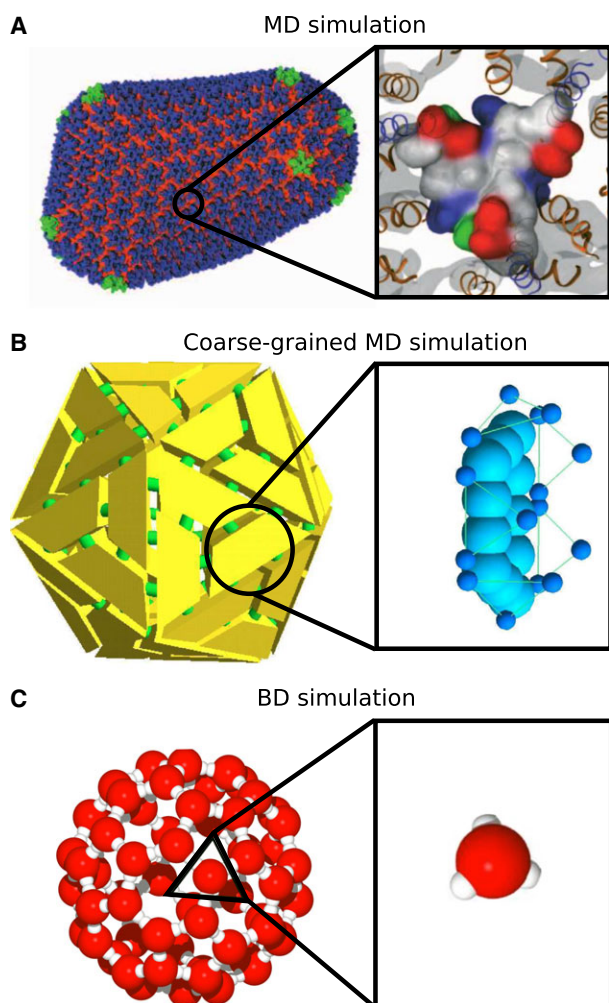


Fig. 3. Modeling virus capsid assembly with different simulation techniques. (A) All-atom molecular dynamics (MD) simulation with the NAMD simulation software of a HIV-1 capsid consisting of 64 million atoms. The capsid comprises 216 hexamers (blue, orange) and 12 pentamers (green). The magnification shows a trimer interface with atomistic details. Left and right subfigure reprinted by permission from Macmillan Publishers Ltd: Nature [51], © (2013). (B) Complete assembly of a T-1 capsid consisting of 60 capsomeres, which form 12 pentamers and 20 hexamers, in a coarse-grained MD-simulation. Single capsomeres (yellow) are reduced in size to visualize bonds (green) between capsomeres. The magnification shows the model of a trapezoidal capsomere with reduced level of detail. Large spheres represent shape whereas small spheres represent interaction sites. Reprinted left and right subfigure with permission from [49] © (2004) by the American Physical Society. (C) Complete assembly of a T-1 capsid in a Brownian Dynamics simulation with patchy particles. The magnification shows the model of a single capsomere (red) with three reactive patches (white). Courtesy of Heinrich Klein.

mann distribution) [56] or Brownian dynamics (BD) simulations (where the effect of the aqueous medium is represented by stochastic noise) (Fig. 3C) [57].

BD-simulations become very efficient if only short-ranged interactions between reaction patches are taken into account [57,58]. On an even more coarse-grained level, one can use stochastic simulations for the growth of the lattice without continuous spatial degrees of freedom [59–61]. If one focuses on equilibrium properties of assembly, thermodynamic models based on the law of mass action can be used [62].

The most important insight that has emerged from these studies is that for successful capsid assembly dissociation events are as important as association events. In other words, the strength of the binding interactions between the capsomeres has to be intermediate [7]. Weak capsomere interactions do not allow for the formation of large clusters, whereas strong capsomere interactions foster the occurrence of stable intermediates that can neither assemble to full capsids nor decay to smaller intermediates. As a result, the system is kinetically trapped. A similar problem has to be solved in the context of protein folding. An additional interesting analogy to protein folding, which often is assisted by chaperones, is that it has been observed for many virus types that scaffold proteins assist kinetically and thermodynamically in the capsid assembly [63]. Recently, it has been argued that another important mechanism to avoid kinetic trapping is the fact that in practice new capsomeres are supplied with a certain rate to the assembly process [58,61]. Another interesting feature observed in the different modeling approaches is the occurrence of a lag phase, which is required for the system to prepare for the growth phase by assembling the right mix of intermediates [63]. These results in fact agree well with the classical theory of nucleation and growth [64–66].

The replication within—intracellular processes

Understanding the dynamics of viral infection and spread on a cellular level requires the combined analysis of the underlying processes, such as viral entry, transport, replication, virus packaging and viral export, assembled into one kinetic scheme. Population dynamic models providing such a systematic analysis need to cover the pathogen-specific intracellular life cycle but face the challenge of balancing model complexity and available data to provide reasonable conclusions on the pathogen dynamics.

Modeling the intracellular viral life cycle

One of the earliest models taking an integrative view at the biochemical processes involved in intracellular

viral integration and gene expression during infection by HIV-1 was developed by Hammond [67] roughly 12 years after the discovery of the virus. They described the central intracellular processes of viral transcription, splicing and translation by a system of coupled ordinary differential equations (ODEs) involving 19 parameters determining the dynamics. This study was followed by an even more detailed model covering the whole intracellular HIV-1 life cycle from reverse transcription over integration and translation to viral assembly and export [68]. Both studies were able to provide a qualitative prediction of the impact of certain processes on the overall dynamics and found sets of parameters that were able to reproduce *in vitro* data of HIV-1 DNA and RNA synthesis [69]. These models and other studies [70] represent a first attempt to quantitate intracellular replication processes in detail. However, due to the limited amount of data and the complexity of their models, the expressiveness of the estimated rate constants quantitating the biochemical processes was limited.

In comparison to HIV-1, more attempts to quantitate intracellular processes using dynamical models have been made for hepatitis C virus (HCV). The development of the HCV replicon system that allowed studying HCV replication *in vitro* [71] improved our understanding of relevant steps within the life cycle of this particular virus and also fostered the development of mathematical models quantitating these intracellular processes. Dahari *et al.* [72] developed a first detailed model on the subgenomic processes involved in HCV replication. In contrast to Reddy and Yin [68], who separated between the nucleus and the cytoplasm to model HIV infection, Dahari *et al.* [72] modeled processes in the vesicular membrane structures (VSM) and the cytoplasm, assuming that HCV synthesis occurs in VSM and that replication involved a double-stranded RNA intermediate. Based on a qualitative comparison of their model to *in vitro* data [71,73], they found that an observed $\sim 10 : 1$ ratio between plus- to minus-strand RNA can be explained by a ~ 200 -fold higher affinity of HCV NS5B polymerase-containing replication complexes to minus-strand RNA, and that the number of transfected HCV plus-strand RNAs changed the time to reach a steady state but did not affect its level. The model by Dahari *et al.* [72] provided a first important step toward understanding HCV replication mechanisms by putting known and hypothesized intracellular processes into a quantitative framework. Applying the same model to viral RNA and protein translation measurements in Huh-7

cell cultures, Binder *et al.* [74] realized that the model needed to be extended to capture the initial dynamics of HCV RNA replication upon early transfection of viral genomes into 'naïve' cells. Considering an additional processing step for transfected RNA and cis-triggered formation of the replication compartment [74], the model was able to reproduce the dynamics observed in the experimental data. Furthermore, they identified a protective replication compartment as essential for sustained RNA replication. By conducting a sensitivity analysis of the model-parameters, they were able to show that if the amount of viral and/or host protein inside the replication compartment is limited, the VSMs are protecting but also attenuating RNA replication, verifying their model predictions on expected behavior of viral mutants by newly performed experiments.

The effect of treatment

As shown by Binder *et al.* [74], mathematical models that systematically describe the key determinants of intracellular viral replication can help to identify sensitive steps of the viral life cycle and, hence, appropriate drug targets for effective intervention. Similarly, mathematical models can be used to reveal treatment effects by identifying the actual mechanism of action of specific drug therapies or by quantitating their effect. For example, Guo *et al.* [75] estimated the half-life of viral HCV RNA *in vitro* under treatment with alpha interferon (IFN- α) to be approximately 12 h. In another study, Dahari *et al.* [76] found a bi-phasic decline in intracellular RNA levels in HCV-infected cells treated with IFN- α . Based on their analysis, they concluded that the viral dynamics observed during *in vitro* experiments under IFN-treatment is not solely due to an enhanced degradation of viral RNA as otherwise the natural half-life of replicons would have to be several days instead of hours. They found that IFN- α primarily acts by reducing RNA production with an additional effect on RNA degradation for doses larger than $250 \text{ U}\cdot\text{mL}^{-1}$ IFN- α . In comparison to Guo *et al.* [75], their estimated half-life of intracellular genotype 1b subgenomic replicon RNA was between 16–19 h. However, Ivanisenko *et al.* [77] showed that the observed bi-phasic RNA decline can also be explained by the accumulation of drug resistant mutants considering stochastic viral mutation and selection in the previous subgenomic model [72]. Two extensive reviews about viral kinetic modeling in the context of treatment with a specific focus on HCV and influenza virus can be found in [78] and [6].

Going live—studying viral replication from clinical data

While *in vitro* experiments provide the opportunity to obtain intracellular measurements in predefined and well-manipulated cell populations, inferring and quantitating intracellular processes from clinical data is much more challenging. Measurements are usually limited to the dynamics of the viral load in plasma or serum of a patient over time. Convolution of connected intracellular processes into single parameters is needed to make quantitative inferences on viral replication.

The standard model of viral dynamics (SMV) [79] is a kinetic model describing the coupled time course of different populations (see Box 1 and Fig. 4). In this model, the intracellular processes of transcription, assembly and export are combined in the viral production rate, ρ , i.e., the number of viral particles produced by one productively infected cell over time. Applying this model and various extensions thereof to viral load data from infected patients under treatment provided important insights into HIV-1 and HCV replication dynamics. Perelson *et al.* [2] and Wei *et al.* [80] were the first to show that HIV-1 replicated extensively during the chronic infection phase. They estimated an average total HIV-1 production per patient of 10.3×10^9 virions per day, which was substantially higher than previous estimates, and a viral half-life in plasma of $t_{1/2} = 0.24$ days [2]. Analogously, the viral half-life of HCV was estimated to be $t_{1/2} = 2.7$ h (range 1.5–4.6 h) with a total production of 1.28×10^{12} virions per day per patient (standard deviation: 4.98×10^{11}) [81] (Table 1). For HIV-1, the model was able to explain the short-term dynamics of the viral load after initiation of antiretroviral treatment (ART) with reverse transcriptase inhibitors that block the ability of HIV-1 to infect other cells, and protease inhibitors that cause the production of noninfectious viral particles [2]. The long-term dynamics, which the model fell short to capture, could be explained by additional long-lived infected cell populations, such as resting memory CD4⁺ T cells, with slower rates of viral turnover [82].

Several extensions to the standard model have been made to account for additional processes, such as intracellular delay [83,84], multiple infection of target cells [85], and viral mutations [86–88]. Some of the model extensions including more sophisticated approximations of the intracellular replication cycle [86,89] allowed a theoretical analysis of expected infection dynamics and disease progression while not being appropriate to quantitate actual processes. These

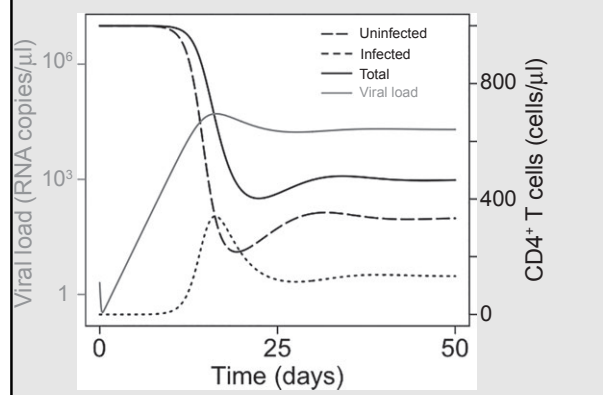
Box 1. The standard model of viral dynamics considers the change in the density of susceptible target cells (T), infected cells (I) and the virus load (V) over time. Target cells enter the system at a continuous rate λ and have an average lifetime of 1/day. Target cells become infected at a rate β proportional to the concentration of free virions, and infected cells die with rate δ . Virions are produced by infected cells at a constant rate ρ and are cleared from the system with a viral clearance rate c . The system of ordinary differential equations describing the dynamics is shown in the following:

$$dT/dt = \lambda - dT - \beta VT$$

$$dI/dt = \beta VT - \delta I$$

$$dV/dt = \rho I - cV$$

The model assumes that viral growth is confined by target cell limitation, and that target cells and virions are well-mixed. Intracellular processes, such as viral transcription, assembly and export are convoluted in single, time-constant rates, as e.g., the viral production rate ρ . There have been various extensions to the standard model of viral dynamics, such as the consideration of an eclipse phase by distinguishing between nonproductively and productively infected cells (Fig. 4 and [83]), or the consideration of treatment [6]. Parameters characterizing viral replication and turn over can be estimated by fitting the model, or adaptations thereof, to viral load data [79]. The plot shows the typical time course for the early phase of an HIV-1 infection predicted with parameter values as given in Table 1.



models helped to identify conditions under which drug resistant mutants arise [84,86,89], and identified appropriate targets for drug treatment [84]. Further extensions to the standard model allowed the analysis and

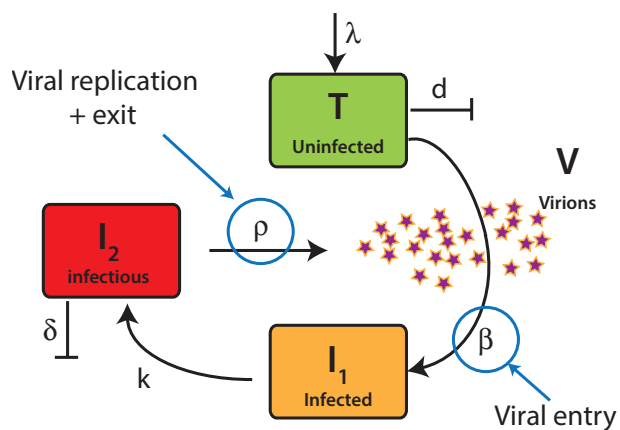


Fig. 4. The extended standard model of viral dynamics distinguishing between the concentrations of uninfected (T , green), infected (I_1 , orange) and infectious (I_2 , red) cells, as well as of the viral load (V). Individual subprocesses, such as viral entry or viral replication and export are convoluted within the rates of viral transmission, β , or the viral production rate, ρ , respectively (see also Box 1 and Table 1). Estimates for these rates can be compared to results from analyses of more detailed models, as e.g., for subgenomic viral replication on *in vitro* data.

quantitation of intracellular processes in more detail. For example, one accounted for the so-called eclipse phase, i.e., the time for integration and translation of

the virus, before actual virus production can be observed by distinguishing between nonproductively and productively infected, i.e., infectious, cells (Fig. 4) [90]. Other models considered time-dependent rates for viral replication, production and clearance, e.g., assuming that viral production depends on the time a cell has been infected [83,91,92]. Using such age-structured models, it was shown that observed viral progression dynamics of HIV-1 infected patients [2] are consistent with the assumption of an exponential increase in viral production with the age of infection of a cell [83], which was also suggested for other pathogens [93,94]. Accounting for time-dependency of intracellular processes, the lifespan of HIV-1 infected cells might be even shorter than previous estimates of 1–2 days (Table 1). However, the actual turnover of HIV-1 within a patient was independent of the kinetic profile of virus production [83,91]. By an even more detailed age-structured multiscale model also considering the level of intracellular viral RNA [5,84] the actual mechanism of daclatasvir, i.e., a direct-acting antiviral agent against HCV, on HCV virus dynamics could be determined. With their analysis, Guedj *et al.* [5] suggested that daclatasvir mediates its antiviral effect by blocking viral RNA synthesis and inhibiting virion assembly/secretion with a mean effectiveness of > 99%. In addition, they were able to provide a more

Table 1. Estimated parameters for the replication and spread of HIV and HCV obtained from the combination of mathematical modeling and experimental and clinical data. Sometimes, obtained quantities can vary over orders of magnitude due to experimental systems and mathematical models used.

Description	Parameter	Unit	Value	Data	Ref.
HIV					
Infection rate	β	(TCID ₅₀ /ml) ⁻¹ day ⁻¹ (SHIV)	4.95 [2.35–9.59] ($\times 10^{-5}$)	<i>In vitro</i>	[125]
Death rate of infected cells	δ	day ⁻¹	0.48–1.36 \pm 0.16	<i>In vivo</i>	[2,83]
			1.18 [0.85–1.26]	<i>In vitro</i>	[125]
Duration of eclipse phase	1/k	h	~ 2–18	<i>In vivo</i>	[83]
Viral production rate	ρ	Virions cell ⁻¹ day ⁻¹ (SIV)	~ 0.7–3.4 ($\times 10^3$)	<i>In vivo</i>	[93,114]
		Virions cell ⁻¹ day ⁻¹ (SIV)	5.0 [1.3–12.0] ($\times 10^4$)	<i>In vivo</i>	[124]
Total production rate	ρ^*/l	Virions day ⁻¹ (HIV)	10.3 \pm 11.7 ($\times 10^9$)	<i>In vivo</i>	[2,4]
Viral clearance rate	c	day ⁻¹	3.07 \pm 0.64	<i>In vivo</i>	[2]
		day ⁻¹	~ 23.0	<i>In vivo</i>	[4]
		day ⁻¹ (SIV)	245–331	<i>In vivo</i>	[115]
HCV					
Death rate of infected cells	δ	day ⁻¹	0.14 \pm 0.13	<i>In vivo</i>	[81]
			1.06 \pm 0.25	<i>In vivo</i>	[5]
Viral production rate					
Total production rate	ρ^*/l	Virions day ⁻¹	1.28 \pm 0.50 ($\times 10^{12}$)	<i>In vivo</i>	[81]
Intracellular model					
Viral export rate	ρ	RNA+ day ⁻¹	8.18 \pm 1.8	<i>In vivo</i>	[5]
Viral RNA degradation rate	μ	day ⁻¹	1.46 \pm 0.36	<i>In vivo</i>	[5]
		day ⁻¹	~ 1.4	<i>In vitro</i>	[75]
Viral clearance rate	c	day ⁻¹	6.2 \pm 1.8	<i>In vivo</i>	[81]
			22.3 \pm 1.7	<i>In vivo</i>	[5]

detailed estimate for serum HCV half-life of 45 min, compared to 2.7 h estimated previously [81].

In summary, the previous examples show how the combination of experimental and clinical data with appropriate mathematical models allows us to quantify key processes of intracellular viral replication even when only measuring at the cellular level.

Viral spread at tissue levels—an integrated view

The standard model of viral dynamics (see Box 1) represents a basic framework to analyze the dynamics of viral infections while spreading through a population of cells. In combination with clinical and experimental data, this model was able to provide quantitative insights into the dynamics of viral infections as outlined before and reviewed in [79]. Besides the convolution of intracellular processes within single parameters, one main characteristic of the SMV is the assumption of well-mixed homogeneous populations of target cells and viral particles. This allows us to quantitate average infection dynamics at the level of the organism. However, such a model neither accounts for spatial aspects of viral spread nor for heterogeneous cell populations, such as cells in different organs, which might differ in their infection dynamics. In case these aspects are of particular interest for the questions addressed, other approaches are needed to analyze the particular dynamics.

Cell-to-cell transmission

As experimental methods improved, it became obvious that many pathogens, such as HIV-1 and HCV, could not only infect cells by cell-free virions, but that infection is also transmitted via direct cell-to-cell contacts [1]. Different mechanisms of this direct cell-to-cell transmission of viral material from infected to uninfected neighbors could be observed, including viral synapses and transport via tight junctions [1]. While the exact contribution of cell-free and cell-to-cell transmission to infection *in vivo* is still undetermined for several pathogens, such as HIV-1 and HCV, it becomes more and more evident that cell-to-cell transmission plays an important, if not a major role for viral spread [95,96]. Therefore, accounting for these two modes of viral transmission when analyzing and quantitating viral replication dynamics becomes important, especially when studying infection dynamics within solid tissues. It was shown theoretically that neglecting spatial aspects can lead to distinct dynamics [97] and to the underestimation of the true infection

dynamics [98]. A recent study incorporated both modes of transmission within a dynamic model allowing for transmission by either infected cells or free virions [99]. With this model, they were able to recapitulate general disease dynamics in HIV-1 infected patients and predicted the effect of short-pulse ART. They found that cell-to-cell spread is an important feature to establish infection, and a relevant drug target to improve disease outcome [99]. Cell-to-cell and cell-free spreading complement each other and allow effective spread of the infection. Using a similar model, Iwami *et al.* [100] estimated that cell-to-cell transmission accounts for roughly 60% of the infection within *in vitro* HIV-1 cell cultures. They also estimated a ~4-fold higher fitness of this mode of transmission compared to cell-free spread, and a 0.9-fold shorter viral generation time, emphasizing the enhanced efficacy. Other studies even estimated cell-to-cell transmission to be 100–18 000 times more effective than cell-free transmission [96,101].

While the previously introduced models [99,100] seem to be appropriate for analyzing data describing large scale dynamics and having motile, diffusive cell populations, they are inappropriate when one is interested in local spreading behavior and/or in pathogens spreading within solid tissues, such as HCV within the liver. Within solid tissue environments, spread by cell-to-cell transmission only allows infection of neighboring cells, thus can lead to foci of infected cells and the infection moving like a traveling wave through the tissue as shown by computational models [102,103].

Recent advances in combining visualization techniques and viral quantitation methods provide the necessary data to obtain quantitative information of the processes involved in cell-to-cell transmission [10]. Analyzing spatial patterns of infected cells obtained by laser capture microdissection within liver biopsy samples of HCV-infected patients, it was found that HCV tends to occur in small clusters containing 4–50 infected cells [10,104]. This suggests that HCV effectively exploits both modes of transmission with clusters being seeded by diffusing virions followed by preferential local spread, such as cell-to-cell transmission [10,104]. Combining spatial information and intracellular viral load using a model for intracellular viral replication, it was estimated that HCV-infected cells could have a fast turnover with cells in a cluster being infected for less than a week [104]. However, this estimate neglected possible immune modulatory effects inhibiting viral replication and therefore serves as a lower bound. Analyzing *in vitro* HCV spread assays, Graw *et al.* [105] estimated that HCV infected Huh 7.5 cells infect other cells by cell-to-cell transmis-

sion with a rate of $\sim 3\text{--}6 \times 10^{-2} \text{ h}^{-1}$. In addition, they found a hierarchy of efficacies when blocking specific HCV entry receptors. Comparable estimates for HCV cell-free infection rates or combined infection rates are lacking as most quantitative information has been obtained from patients under antiviral treatment [81].

The mode of transmission might also influence intracellular replication and evolutionary dynamics at the tissue level. Cell-to-cell transmission offers the possibility to introduce many viral genomes into neighboring cells [1]. Del Portillo *et al.* [106] showed that cell-to-cell infection of target cells with HIV *in vitro* does not follow a Poisson distribution in contrast to cell-free infection and concluded that the cell-to-cell infection process can transmit a variable number of genomes to the target cells. As shown by integrative computational simulations and experimental data for a plant virus [107], stochastic variation in the number of genomes starting viral replication per cell and heterogeneity in the accumulation of viral progenies among strains allows rapid adaptation of the virus to the environment, although viral replication is started by less than 20 founder genomes. Mathematical models also predict that the transmission of variable numbers of viral particles by cell-to-cell transmission influences the efficacy of viral replication and the susceptibility of infection to antiviral drugs [108,109].

Based on previous methods applied to problems in ecology and evolution, there have been other modeling attempts to study the spatial spread of an infection within a host organism. These different methods include partial differential equations [110] and cell-centered or agent-based models [102,111,112]. Agent-based models simulate ensembles of individual cells in time and space. They are able to represent detailed information on internal cell states and contributed to our understanding of disease pathology and immunology [111]. These models can also address the spatial interaction of cells in various levels of detail, e.g., modeling cells as cubes or spheres on a lattice (e.g., cellular automata [102,111]), or modeling cells comprising several lattice sites and changing size as a function of mechanical and adhesive properties (e.g., cellular Potts model [113]). Because of their complexity and their dependence on a large set of unknown parameters, these models have been mostly used to analyze the qualitative behavior of viral spread and the dependence on specific parameters [102] and mechanisms [112]. As experimental methods improve and more quantitative data become available, these sophisticated methods can be used to obtain quantitative estimates of the spatial aspects of viral dynamics.

Heterogeneous cell populations

Another important feature not represented by the standard model of viral dynamics is the existence of heterogeneous cell populations that vary in their replication kinetics and behavior. Compartmentalization has been used to obtain organ-specific replication and clearance rates of Simian immunodeficiency virus (SIV), the monkey equivalent of HIV [114,115], an important aspect when evaluating the efficacy of drugs with organ-specific pharmacokinetics. Assuming viral burst sizes of 5×10^4 virions [96], they estimated that the clearance rates of SIV in lymphoid organs should be fast (around $c = 50\text{--}500 \text{ day}^{-1}$). In contrast, previous estimates of viral clearance rates in the blood, which are substantially lower, most likely represent virus efflux rates from the blood into other organs. With a similar quantitative argument, Lay *et al.* [116] addressed the question if the gut is the major source of viral replication during early SIV infection. They showed that although cells in the intestinal mucosa are highly susceptible to infection, they are not the main contributors to plasma viral load. These examples indicate how additional information and mathematical modeling helps to disentangle previous estimates averaging different dynamics, and how it improves interpretation of measured quantities on the level of an organism.

Conclusions and outlook

The combination of quantitative experimental and clinical data with mathematical models and computer simulations has substantially advanced our understanding of the dynamics of viral replication and spread. In addition to HIV-1 and HCV, similar analyses as described above have been used to study the infection dynamics of other human and animal viruses, including influenza A [117–119], hepatitis B virus [120–122] and SIV [123–125]. Furthermore, these techniques can also be adapted to the study of multicellular pathogens, such as the malaria causing parasite *Plasmodium falciparum* [126].

Analyzing the relevant intra- and intercellular processes with biophysical concepts and methods as well as with population dynamic arguments allows us to combine information across multiple scales in space and time. The rapid pace of current experimental advances promises to soon fill many more gaps in our understanding of viral dynamics. Improved imaging techniques from single molecule tracking to two-photon microscopy in tissue, as well as 3D cell and tissue cultures of increased complexity will advance the

possibility to observe and quantitate dynamical processes in the required detail, and to reveal potential targets for therapeutic interventions (reviewed in [127] and [128]). In addition, they allow studying the combined interaction of pathogen replication and host responses [127], an additional level of complexity that has also been considered by mathematical models [79], but was not addressed in this review. Besides providing additional information on infection dynamics, the novel types of data will also represent additional challenges for mathematical modeling, i.e., to incorporate them within a systematic and quantitative framework. On the long run, however, this effort will pay off with a systems-level understanding that can then quickly be adapted for new situations of biological and medical interest.

Acknowledgements

PK and FG are supported by the Center for Modeling and Simulation in the Biosciences (BIOMS). FF acknowledges support by the Heidelberg Graduate School for Fundamental Physics (HGSFP). USS is a member of the cluster of excellence CellNetworks, and USS and FG are members of the Interdisciplinary Center for Scientific Computing (IWR).

Author contributions

USS and FG conceived the review. PK, FF, USS and FG wrote the manuscript.

References

- Sattentau Q (2008) Avoiding the void: cell-to-cell spread of human viruses. *Nat Rev Microbiol* **6**, 815–826.
- Perelson AS, Neumann AU, Markowitz M, Leonard JM and Ho DD (1996) HIV-1 dynamics in vivo: virion clearance rate, infected cell life-span, and viral generation time. *Science* **271**, 1582–1586.
- Ho DD, Neumann AU, Perelson AS, Chen W, Leonard JM and Markowitz M (1995) Rapid turnover of plasma virions and CD4 lymphocytes in HIV-1 infection. *Nature* **373**, 123–126.
- Ramratnam B, Bonhoeffer S, Binley J, Hurley A, Zhang L, Mittler JE, Markowitz M, Moore JP, Perelson AS and Ho DD (1999) Rapid production and clearance of HIV-1 and hepatitis C virus assessed by large volume plasma apheresis. *Lancet* **354**, 1782–1785.
- Guedj J, Dahari H, Rong L, Sansone ND, Nettles RE, Cotler SJ, Layden TJ, Uprichard SL and Perelson AS (2013) Modeling shows that the NS5A inhibitor daclatasvir has two modes of action and yields a shorter estimate of the hepatitis C virus half-life. *Proc Natl Acad Sci USA* **110**, 3991–3996.
- Chatterjee A, Smith PF and Perelson AS (2013) Hepatitis C viral kinetics: the past, present, and future. *Clin Liver Dis* **17**, 13–26.
- Hagan MF (2014) Modeling viral capsid assembly. *Adv Chem Phys* **155**, 1–68.
- Shulla A and Randall G (2015) Spatiotemporal analysis of hepatitis C virus infection. *PLoS Pathog* **11**, e1004758.
- von Schaeuwen M, Ding Q and Ploss A (2014) Visualizing hepatitis C virus infection in humanized mice. *J Immunol Methods* **410**, 50–59.
- Kandathil AJ, Graw F, Quinn J, Hwang HS, Torbenson M, Perelson AS, Ray SC, Thomas DL, Ribeiro RM and Balagopal A (2013) Use of laser capture microdissection to map hepatitis C virus-positive hepatocytes in human liver. *Gastroenterology* **145**, 1404–1413.
- Radtke K, Döhner K and Sodeik B (2006) Viral interactions with the cytoskeleton: a hitchhiker's guide to the cell. *Cell Microbiol* **8**, 387–400.
- Fackler OT and Kräusslich H-G (2006) Interactions of human retroviruses with the host cell cytoskeleton. *Curr Opin Microbiol* **9**, 409–415.
- Marsh M and Helenius A (2006) Virus entry: open sesame. *Cell* **124**, 729–740.
- Pelkmans L (2005) Viruses as probes for systems analysis of cellular signalling, cytoskeleton reorganization and endocytosis. *Curr Opin Microbiol* **8**, 331–337.
- Brandenburg B and Zhuang X (2007) Virus trafficking – learning from single-virus tracking. *Nat Rev Microbiol* **5**, 197–208.
- Greber UF and Way M (2006) A superhighway to virus infection. *Cell* **124**, 741–754.
- Lukinavičius G, Reymond L, D'Este E, Masharina A, Göttfert F, Ta H, Güther A, Fournier M, Rizzo S, Waldmann H *et al.* (2014) Fluorogenic probes for live-cell imaging of the cytoskeleton. *Nat Methods* **11**, 731–733.
- Wu YI, Frey D, Lungu OI, Jaehrig A, Schlichting I, Kuhlman B and Hahn KM (2009) A genetically encoded photoactivatable Rac controls the motility of living cells. *Nature* **461**, 104–108.
- Magnus C, Rusert P, Bonhoeffer S, Trkola A and Regoes RR (2009) Estimating the stoichiometry of human immunodeficiency virus entry. *J Virol* **83**, 1523–1531.
- Brandenberg OF, Magnus C, Rusert P, Regoes RR and Trkola A (2015) Different infectivity of HIV-1 strains is linked to number of envelope trimers required for entry. *PLoS Pathog* **11**, e1004595.

- 21 Padmanabhan P and Dixit NM (2011) Mathematical model of viral kinetics in vitro estimates the number of E2-CD81 complexes necessary for hepatitis C virus entry. *PLoS Comput Biol* **7**, e1002307.
- 22 Lehmann MJ, Sherer NM, Marks CB, Pypaert M and Mothes W (2005) Actin- and myosin-driven movement of viruses along filopodia precedes their entry into cells. *J Cell Biol* **170**, 317–325.
- 23 Daecke J, Fackler OT, Dittmar MT and Kräusslich H-G (2005) Involvement of clathrin-mediated endocytosis in human immunodeficiency virus type 1 entry. *J Virol* **79**, 1581–1594.
- 24 McDonald D, Vodicka MA, Lucero G, Svitkina TM, Borisy GG, Emerman M and Hope TJ (2002) Visualization of the intracellular behavior of HIV in living cells. *J Cell Biol* **159**, 441–452.
- 25 Bressloff PC and Newby JM (2013) Stochastic models of intracellular transport. *Rev Mod Phys* **85**, 135–196.
- 26 Lagache T, Dauty E and Holcman D (2009) Physical principles and models describing intracellular virus particle dynamics. *Curr Opin Microbiol* **12**, 439–445.
- 27 Schuss Z, Singer A and Holcman D (2007) The narrow escape problem for diffusion in cellular microdomains. *Proc Natl Acad Sci USA* **104**, 16098–16103.
- 28 Seisenberger G, Ried MU, Endreß T, Büning H, Hallek M and Bräuchle C (2001) Real-time single-molecule imaging of the infection pathway of an adeno-associated virus. *Science* **294**, 1929–1932.
- 29 Nakano MY and Greber UF (2000) Quantitative microscopy of fluorescent adenovirus entry. *J Struct Biol* **129**, 57–68.
- 30 Dinh A-T, Theofanous T and Mitragotri S (2005) A model for intracellular trafficking of adenoviral vectors. *Biophys J* **89**, 1574–1588.
- 31 Lipowsky R and Klumpp S (2005) ‘Life is motion’: multiscale motility of molecular motors. *Phys A* **352**, 53–112.
- 32 Guérin T, Prost J, Martin P and Joanny J-F (2010) Coordination and collective properties of molecular motors: theory. *Curr Opin Cell Biol* **22**, 14–20.
- 33 Klumpp S and Lipowsky R (2005) Cooperative cargo transport by several molecular motors. *Proc Natl Acad Sci USA* **102**, 17284–17289.
- 34 Müller MJ, Klumpp S and Lipowsky R (2008) Tug-of-war as a cooperative mechanism for bidirectional cargo transport by molecular motors. *Proc Natl Acad Sci USA* **105**, 4609–4614.
- 35 Gao H, Shi W and Freund LB (2005) Mechanics of receptor-mediated endocytosis. *Proc Natl Acad Sci USA* **102**, 9469–9474.
- 36 Sun SX and Wirtz D (2006) Mechanics of enveloped virus entry into host cells. *Biophys J* **90**, L10–L12.
- 37 Dasgupta S, Auth T and Gompper G (2014) Shape and orientation matter for the cellular uptake of nonspherical particles. *Nano Lett* **14**, 687–693.
- 38 Tzllil S, Deserno M, Gelbart WM and Ben-Shaul A (2004) A statistical-thermodynamic model of viral budding. *Biophys J* **86**, 2037–2048.
- 39 Roos WH, Bruinsma R and Wuite GJL (2010) Physical virology. *Nat Phys* **6**, 733–743.
- 40 Fraenkel-Conrat H and Williams RC (1955) Reconstitution of active tobacco mosaic virus from its inactive protein and nucleic acid components. *Proc Natl Acad Sci USA* **41**, 690–698.
- 41 Crick FHC and Watson JD (1956) Structure of small viruses. *Nature* **177**, 473–475.
- 42 Caspar DLD and Klug A (1962) Physical principles in the construction of regular viruses. *Cold Spring Harb Symp Quant Biol* **27**, 1–24.
- 43 Sundquist WI and Kräusslich H-G (2012) HIV-1 assembly, budding, and maturation. *Cold Spring Harb Perspect Med* **2**, a006924.
- 44 Kler S, Asor R, Li C, Ginsburg A, Harries D, Oppenheim A, Zlotnick A and Raviv U (2012) RNA encapsidation by SV40-derived nanoparticles follows a rapid two-state mechanism. *J Am Chem Soc* **134**, 8823–8830.
- 45 JaG Briggs, Riches JD, Glass B, Bartonova V, Zanetti G and Kräusslich H-G (2009) Structure and assembly of immature HIV. *Proc Natl Acad Sci USA* **106**, 11090–11095.
- 46 Han Y, Ahn J, Concel J, Byeon I-JL, Gronenborn AM, Yang J and Polenova T (2010) Solid-state NMR studies of HIV-1 capsid protein assemblies. *J Am Chem Soc* **132**, 1976–1987.
- 47 Hagan MF and Chandler D (2006) Dynamic pathways for viral capsid assembly. *Biophys J* **91**, 42–54.
- 48 Uetrecht C, Barbu IM, Shoemaker GK, van Duijn E and Albert AJR (2011) Interrogating viral capsid assembly with ion mobility–mass spectrometry. *Nat Chem* **3**, 126–132.
- 49 Rapaport DC (2004) Self-assembly of polyhedral shells: a molecular dynamics study. *Phys Rev E* **70**, 051905.
- 50 Freddolino PL, Arkhipov AS, Larson SB, McPherson A and Schulten K (2006) Molecular dynamics simulations of the complete satellite tobacco mosaic virus. *Structure* **14**, 437–449.
- 51 Zhao G, Perilla JR, Yufenyuy EL, Meng X, Chen B, Ning J, Ahn J, Gronenborn AM, Schulten K, Aiken C *et al.* (2013) Mature HIV-1 capsid structure by cryo-electron microscopy and all-atom molecular dynamics. *Nature* **497**, 643–646.
- 52 Phillips JC, Braun R, Wang W, Gumbart J, Tajkhorshid E, Villa E, Chipot C, Skeel RD, Kale L and Schulten K (2005) Scalable molecular dynamics with NAMD. *J Comput Chem* **26**, 1781–1802.
- 53 Berendsen HJC, van der Spoel D and van Drunen R (1995) GROMACS: a message-passing parallel

- molecular dynamics implementation. *Comput Phys Commun* **91**, 43–56.
- 54 Shepherd CM, Borelli IA, Lander G, Natarajan P, Siddavanahalli V, Bajaj C, Johnson JE, Brooks CL and Reddy VS (2006) VIPERdb: a relational database for structural virology. *Nucleic Acids Res* **34**, D386–D389.
- 55 Rapaport DC, Johnson JE and Skolnick J (1999) Supramolecular self-assembly: molecular dynamics modeling of polyhedral shell formation. *Comput Phys Commun* **121–122**, 231–235.
- 56 Wilber AW, Doye JPK, Louis AA, Noya EG, Miller MA and Wong P (2007) Reversible self-assembly of patchy particles into monodisperse icosahedral clusters. *J Chem Phys* **127**, 085106.
- 57 Baschek JE, Klein HCR and Schwarz US (2012) Stochastic dynamics of virus capsid formation: direct versus hierarchical self-assembly. *BMC Biophys* **5**, 22.
- 58 Boettcher MA, Klein HCR and Schwarz US (2015) Role of dynamic capsomere supply for viral capsid self-assembly. *Phys Biol* **12**, 16014.
- 59 Berger B, Shor PW, Tucker-Kellogg L and King J (1994) Local rule-based theory of virus shell assembly. *Proc Natl Acad Sci USA* **91**, 7732–7736.
- 60 Xie L, Smith GR, Feng X and Schwartz R (2012) Surveying capsid assembly pathways through simulation-based data fitting. *Biophys J* **103**, 1545–1554.
- 61 Dykeman EC, Stockley PG and Twarock R (2014) Solving a Levinthal's paradox for virus assembly identifies a unique antiviral strategy. *Proc Natl Acad Sci USA* **111**, 5361–5366.
- 62 Zlotnick A (1994) To build a virus capsid: an equilibrium model of the self assembly of polyhedral protein complexes. *J Mol Biol* **241**, 59–67.
- 63 Zlotnick A and Mukhopadhyay S (2011) Virus assembly, allostery and antivirals. *Trends Microbiol* **19**, 14–23.
- 64 Prevelige PE, Thomas D and King J (1993) Nucleation and growth phases in the polymerization of coat and scaffolding subunits into icosahedral procapsid shells. *Biophys J* **64**, 824–835.
- 65 Zandi R, van der Schoot P, Reguera D, Kegel W and Reiss H (2006) Classical nucleation theory of virus capsids. *Biophys J* **90**, 1939–1948.
- 66 Hagan MF and Elrad OM (2010) Understanding the concentration dependence of viral capsid assembly kinetics—the origin of the lag time and identifying the critical nucleus size. *Biophys J* **98**, 1065–1074.
- 67 Hammond BJ (1993) Quantitative study of the control of HIV-1 gene expression. *J Theor Biol* **163**, 199–221.
- 68 Reddy B and Yin J (1999) Quantitative intracellular kinetics of HIV type 1. *AIDS Res Hum Retroviruses* **15**, 273–283.
- 69 Berkhout B, Gatignol A, Rabson AB and Jeang KT (1990) TAR-independent activation of the HIV-1 LTR: evidence that tat requires specific regions of the promoter. *Cell* **62**, 757–767.
- 70 Kim H and Yin J (2005) Robust growth of human immunodeficiency virus type 1 (HIV-1). *Biophys J* **89**, 2210–2221.
- 71 Lohmann V, Korner F, Koch J, Herian U, Theilmann L and Bartenschlager R (1999) Replication of subgenomic hepatitis C virus RNAs in a hepatoma cell line. *Science* **285**, 110–113.
- 72 Dahari H, Ribeiro RM, Rice CM and Perelson AS (2007) Mathematical modeling of subgenomic hepatitis C virus replication in Huh-7 cells. *J Virol* **81**, 750–760.
- 73 Quinkert D, Bartenschlager R and Lohmann V (2005) Quantitative analysis of the hepatitis C virus replication complex. *J Virol* **79**, 13594–13605.
- 74 Binder M, Sulaimanov N, Clausnitzer D, Schulze M, Huber CM, Lenz SM, Schloder JP, Trippler M, Bartenschlager R, Lohmann V *et al.* (2013) Replication vesicles are load- and choke-points in the hepatitis C virus lifecycle. *PLoS Pathog* **9**, e1003561.
- 75 Guo JT, Bichko VV and Seeger C (2001) Effect of alpha interferon on the hepatitis C virus replicon. *J Virol* **75**, 8516–8523.
- 76 Dahari H, Sainz B, Perelson AS and Uprichard SL (2009) Modeling subgenomic hepatitis C virus RNA kinetics during treatment with alpha interferon. *J Virol* **83**, 6383–6390.
- 77 Ivanisenko NV, Mishchenko EL, Akberdin IR, Demenkov PS, Likhoshvai VA, Kozlov KN, Todorov DI, Gursky VV, Samsonova MG, Samsonov AM *et al.* (2014) A new stochastic model for subgenomic hepatitis C virus replication considers drug resistant mutants. *PLoS One* **9**, e91502.
- 78 Canini L and Perelson AS (2014) Viral kinetic modeling: state of the art. *J Pharmacokinetic Pharmacodyn* **41**, 431–443.
- 79 Perelson AS (2002) Modelling viral and immune system dynamics. *Nat Rev Immunol* **2**, 28–36.
- 80 Wei X, Ghosh SK, Taylor ME, Johnson VA, Emami EA, Deutsch P, Lifson JD, Bonhoeffer S, Nowak MA and Hahn BH (1995) Viral dynamics in human immunodeficiency virus type 1 infection. *Nature* **373**, 117–122.
- 81 Neumann AU, Lam NP, Dahari H, Gretch DR, Wiley TE, Layden TJ and Perelson AS (1998) Hepatitis C viral dynamics in vivo and the antiviral efficacy of interferon-alpha therapy. *Science* **282**, 103–107.
- 82 Perelson AS, Essunger P, Cao Y, Vesanen M, Hurley A, Saksela K, Markowitz M and Ho DD (1997) Decay characteristics of HIV-1-infected compartments during combination therapy. *Nature* **387**, 188–191.
- 83 Althaus CL, De Vos AS and De Boer RJ (2009) Reassessing the human immunodeficiency virus type 1

- life cycle through age-structured modeling: life span of infected cells, viral generation time, and basic reproductive number, R_0 . *J Virol* **83**, 7659–7667.
- 84 Rong L, Guedj J, Dahari H, Coffield DJ, Levi M, Smith P and Perelson AS (2013) Analysis of hepatitis C virus decline during treatment with the protease inhibitor danoprevir using a multiscale model. *PLoS Comput Biol* **9**, e1002959.
 - 85 Dixit NM and Perelson AS (2005) HIV dynamics with multiple infections of target cells. *Proc Natl Acad Sci USA* **102**, 8198–8203.
 - 86 Althaus CL and De Boer RJ (2012) Impaired immune evasion in HIV through intracellular delays and multiple infection of cells. *Proc Biol Sci* **279**, 3003–3010.
 - 87 Wu H, Huang Y, Dykes C, Liu D, Ma J, Perelson AS and Demeter LM (2006) Modeling and estimation of replication fitness of human immunodeficiency virus type 1 in vitro experiments by using a growth competition assay. *J Virol* **80**, 2380–2389.
 - 88 Ganusov VV, Goonetilleke N, Liu MK, Ferrari G, Shaw GM, McMichael AJ, Borrow P, Korber BT and Perelson AS (2011) Fitness costs and diversity of the cytotoxic T lymphocyte (CTL) response determine the rate of CTL escape during acute and chronic phases of HIV infection. *J Virol* **85**, 10518–10528.
 - 89 Guedj J and Neumann AU (2010) Understanding hepatitis C viral dynamics with direct-acting antiviral agents due to the interplay between intracellular replication and cellular infection dynamics. *J Theor Biol* **267**, 330–340.
 - 90 Beauchemin CA and Handel A (2011) A review of mathematical models of influenza A infections within a host or cell culture: lessons learned and challenges ahead. *BMC Public Health* **11** (Suppl 1), S7.
 - 91 Nelson PW, Gilchrist MA, Coombs D, Hyman JM and Perelson AS (2004) An age-structured model of hiv infection that allows for variations in the production rate of viral particles and the death rate of productively infected cells. *Math Biosci Eng* **1**, 267–288.
 - 92 Rong L, Feng Z and Perelson AS (2007) Emergence of HIV-1 drug resistance during antiretroviral treatment. *Bull Math Biol* **69**, 2027–2060.
 - 93 Reilly C, Wietgreffe S, Sedgewick G and Haase A (2007) Determination of simian immunodeficiency virus production by infected activated and resting cells. *AIDS* **21**, 163–168.
 - 94 Ho DD and Huang Y (2002) The HIV-1 vaccine race. *Cell* **110**, 135–138.
 - 95 Sourisseau M, Sol-Foulon N, Porrot F, Blanchet F and Schwartz O (2007) Inefficient human immunodeficiency virus replication in mobile lymphocytes. *J Virol* **81**, 1000–1012.
 - 96 Chen P, Hubner W, Spinelli MA and Chen BK (2007) Predominant mode of human immunodeficiency virus transfer between T cells is mediated by sustained Env-dependent neutralization-resistant virological synapses. *J Virol* **81**, 12582–12595.
 - 97 Culshaw RV, Ruan S and Webb G (2003) A mathematical model of cell-to-cell spread of HIV-1 that includes a time delay. *J Math Biol* **46**, 425–444.
 - 98 Funk GA, Jansen VA, Bonhoeffer S and Killingback T (2005) Spatial models of virus-immune dynamics. *J Theor Biol* **233**, 221–236.
 - 99 Zhang C, Zhou S, Groppelli E, Pellegrino P, Williams I, Borrow P, Chain BM and Jolly C (2015) Hybrid spreading mechanisms and T cell activation shape the dynamics of HIV-1 infection. *PLoS Comput Biol* **11**, e1004179.
 - 100 Iwami S, Takeuchi JS, Nakaoka S, Mammano F, Clavel F, Inaba H, Kobayashi T, Misawa N, Aihara K, Koyanagi Y *et al.* (2015) Cell-to-cell infection by HIV contributes over half of virus infection. *Elife* **4**, e08150.
 - 101 Sato H, Orenstein J, Dimitrov D and Martin M (1992) Cell-to-cell spread of HIV-1 occurs within minutes and may not involve the participation of virus particles. *Virology* **186**, 712–724.
 - 102 Beauchemin C, Samuel J and Tuszynski J (2005) A simple cellular automaton model for influenza A viral infections. *J Theor Biol* **232**, 223–234.
 - 103 Keeling MJ and Rohani P (2008) Modeling Infectious Diseases in Humans and Animals. Princeton University Press, Princeton, NJ.
 - 104 Graw F, Balagopal A, Kandathil AJ, Ray SC, Thomas DL, Ribeiro RM and Perelson AS (2014) Inferring viral dynamics in chronically HCV infected patients from the spatial distribution of infected hepatocytes. *PLoS Comput Biol* **10**, e1003934.
 - 105 Graw F, Martin DN, Perelson AS, Uprichard SL and Dahari H (2015) Quantification of hepatitis C virus cell-to-cell spread using a stochastic modeling approach. *J Virol* **89**, 6551–6561.
 - 106 Del Portillo A, Tripodi J, Najfeld V, Wodarz D, Levy DN and Chen BK (2011) Multiploid inheritance of HIV-1 during cell-to-cell infection. *J Virol* **85**, 7169–7176.
 - 107 Miyashita S, Ishibashi K, Kishino H and Ishikawa M (2015) Viruses roll the dice: the stochastic behavior of viral genome molecules accelerates viral adaptation at the cell and tissue levels. *PLoS Biol* **13**, e1002094.
 - 108 Komarova NL, Levy DN and Wodarz D (2013) Synaptic transmission and the susceptibility of HIV infection to anti-viral drugs. *Sci Rep* **3**, 2103.
 - 109 Komarova NL and Wodarz D (2013) Virus dynamics in the presence of synaptic transmission. *Math Biosci* **242**, 161–171.

- 110 Strain MC, Richman DD, Wong JK and Levine H (2002) Spatiotemporal dynamics of HIV propagation. *J Theor Biol* **218**, 85–96.
- 111 Bauer AL, Beauchemin CA and Perelson AS (2009) Agent-based modeling of host-pathogen systems: the successes and challenges. *Inf Sci (Ny)* **179**, 1379–1389.
- 112 Murray JM and Goyal A (2015) In silico single cell dynamics of hepatitis B virus infection and clearance. *J Theor Biol* **366**, 91–102.
- 113 Graner F and Glazier JA (1992) Simulation of biological cell sorting using a two-dimensional extended Potts model. *Phys Rev Lett* **69**, 2013–2016.
- 114 De Boer RJ, Ribeiro RM and Perelson AS (2010) Current estimates for HIV-1 production imply rapid viral clearance in lymphoid tissues. *PLoS Comput Biol* **6**, e1000906.
- 115 Zhang L, Dailey PJ, Gettie A, Blanchard J and Ho DD (2002) The liver is a major organ for clearing simian immunodeficiency virus in rhesus monkeys. *J Virol* **76**, 5271–5273.
- 116 Lay MD, Petravic J, Gordon SN, Engram J, Silvestri G and Davenport MP (2009) Is the gut the major source of virus in early simian immunodeficiency virus infection? *J Virol* **83**, 7517–7523.
- 117 Murillo LN, Murillo MS and Perelson AS (2013) Towards multiscale modeling of influenza infection. *J Theor Biol* **332**, 267–290.
- 118 Sidorenko Y and Reichl U (2004) Structured model of influenza virus replication in MDCK cells. *Biotechnol Bioeng* **88**, 1–14.
- 119 Baccam P, Beauchemin C, Macken CA, Hayden FG and Perelson AS (2006) Kinetics of influenza A virus infection in humans. *J Virol* **80**, 7590–7599.
- 120 Ribeiro RM, Lo A and Perelson AS (2002) Dynamics of hepatitis B virus infection. *Microbes Infect* **4**, 829–835.
- 121 Ciupe SM, Ribeiro RM, Nelson PW, Dusheiko G and Perelson AS (2007) The role of cells refractory to productive infection in acute hepatitis B viral dynamics. *Proc Natl Acad Sci USA* **104**, 5050–5055.
- 122 Dahari H, Shudo E, Ribeiro RM and Perelson AS (2009) Modeling complex decay profiles of hepatitis B virus during antiviral therapy. *Hepatology* **49**, 32–38.
- 123 Noecker C, Schaefer K, Zaccaro K, Yang Y, Day J and Ganusov VV (2015) Simple mathematical models do not accurately predict early SIV dynamics. *Viruses* **7**, 1189–1217.
- 124 Chen HY, Di Mascio M, Perelson AS, Ho DD and Zhang L (2007) Determination of virus burst size in vivo using a single-cycle SIV in rhesus macaques. *Proc Natl Acad Sci USA* **104**, 19079–19084.
- 125 Iwami S, Holder BP, Beauchemin CA, Morita S, Tada T, Sato K, Igarashi T and Miura T (2012) Quantification system for the viral dynamics of a highly pathogenic simian/human immunodeficiency virus based on an in vitro experiment and a mathematical model. *Retrovirology* **9**, 18.
- 126 Antia R, Yates A and de Roode JC (2008) The dynamics of acute malaria infections. I. Effect of the parasite's red blood cell preference. *Proc Biol Sci* **275**, 1449–1458.
- 127 Coombes JL and Robey EA (2010) Dynamic imaging of host-pathogen interactions in vivo. *Nat Rev Immunol* **10**, 353–364.
- 128 Fackler OT, Murooka TT, Imle A and Mempel TR (2014) Adding new dimensions: towards an integrative understanding of HIV-1 spread. *Nat Rev Microbiol* **12**, 563–574.